

## Toxicity of silver nanoparticles on virus

Feng Shao

Department of Chemical Engineering, Jinan Institute of Technology, Jinan, China, 250000

Received 21 Sept 2013, Revised 1 Oct 2013, Accepted 1 Oct 2013

\*Corresponding author. Email: [shaofeng1981@163.com](mailto:shaofeng1981@163.com); Tel: 086-13515414334,

### Abstract

This study investigated the antiviral effect of silver nanoparticles on MS2 bacteriophage. Silver nanoparticles were synthesized via chemical reduction method and characterized by transmission electron microscope. Synthesized silver nanoparticles and cultivated MS2 bacteriophage were characterized using zetasizer. The result in this study indicates that the toxicity of silver nanoparticles on MS2 bacteriophage is dose-dependent. Our result show 100 mg/L silver nanoparticles can completely deactivate MS2 bacteriophage.

**Keywords:** silver nanoparticles, MS2 bacteriophage, antiviral effect, toxicity

### 1 Introduction

Among noble-metal nanomaterials, silver nanoparticles (AgNPs) have received considerable attention due to their attractive physicochemical properties [1-8]. The surface plasmon resonance and large effective scattering cross section of individual AgNP make them ideal candidates for molecular labeling [5], where phenomena such as surface enhance Raman scattering (SERS) can be exploited. In addition, the strong toxicity that silver exhibits in various chemical forms to a wide range of microorganisms is very well known [1-8], and AgNPs have recently been shown to be a promising antimicrobial material [4-8].

The antibacterial activities of the AgNP depend on many factors such as particle size, shape, concentration and its aggregation/dissolution in specific growth media [3,6,7]. Recent studies showed that 10 mg/L AgNPs (particle size = 12 nm) reduced *Escherichia coli* growth by 70% [9] while AgNPs (average particle size = 14 nm) caused 55% growth inhibition of *E. coli* PHL628-gfp at a much lower concentration (0.45 mg/L) [8].

Viruses represent an important class of pathogenic nanoparticles in aquatic systems that are responsible for the vast majority of water-borne diseases. Because of this, viruses pose a challenge in removal and disinfection processes for drinking water suppliers. Only recently have studies focused on the importance of biophysical interactions between viruses and interfaces which can be exploited as a method of disinfection or virus removal.

Recent studies shows that AgNPs doped with foamy carbon, poly (N-vinyl-2-pyrrolidone) (PVP), or bovine serum albumin (BSA) can completely killed HIV-1 virus after 24 h treatment at the concentrations more than 10 mg/L [11]. At the concentrations above 12.5 mg/L, the polysaccharide coated AgNPs (particle size around 10 nm) significantly decreased the number of plaque forming units (PFU) of the monkey pox virus (MPV) [12]. These results indicate the potential of using AgNPs at relatively high concentrations (e.g., >10 mg/L Ag) to provide cytoprotective activities towards virusinfected mammal cells. While a wealth of research has demonstrated the antibacterial potential of AgNPs against bacteria, little is known about the antiviral effect of these nanoparticles.

This study aims at investigating the antiviral ability of AgNPs. MS2 bacteriophage was used as a representative virus because it has been extensively studied which allow us to compare our results. AgNPs were synthesized via chemical reduction method and characterized by transmission electron microscopy and dynamic light scattering (DLS). The cultivated MS2 bacteriophage was also characterized by DLS. The surface charge of MS2 virus and AgNP were quantified in terms of zeta potential using zetasizer. Antiviral test was performed using a double agar overlay technique.

### 2 Experimental

AgNPs, with the diameter of approximately 30 nm, were synthesized by the reduction of the complex cation  $[\text{Ag}(\text{NH}_3)_2]^+$  with D-maltose [5]. The initial concentrations of the reaction components were  $1 \times 10^{-3}$  M and

$1 \times 10^{-2}$  M for  $\text{AgNO}_3$  and the reducing sugar, respectively. The concentration of the used ammonia was  $5 \times 10^{-3}$  M. Sodium hydroxide solution was added to the reaction system to adjust the value of pH at about 11.5, as well as to achieve a reaction time of several minutes [5]. Then, stabilizing reagent sodium citrate was added to form stable nanosuspension. The as prepared aqueous dispersion of the AgNPs was used for subsequent experiments without any additional modifications.

*E. coli* bacteriophage MS2 (ATCC 15597-B1), a single-stranded RNA coliphage, was selected as a model virus in this study. The bacteriophage stocks were propagated using the double agar layer (DAL) method. Approximately 100  $\mu\text{L}$  of bacteriophage ( $10^8$  PFU/mL determined by DAL), 200  $\mu\text{L}$  of host bacteria ( $10^8$  CFU/mL determined by standard agar plate method), and 5 mL LB containing 0.5% molten agar (with 0.1% glucose, 2 mM  $\text{CaCl}_2$  and 0.1 mg/mL Thiamine) were poured onto plates containing 1.5% agar. The plates were incubated at  $37^\circ\text{C}$  overnight. The phage stocks were collected the following day by adding 10 mL of  $1 \times$  PBS to the surface of the plate and allowing it to incubate at room temperature for 1 h. The liquid was collected and centrifuged at 3000 rpm for 20 min at room temperature. The supernatant containing the bacteriophage was used as a stock solution (typical MS2 concentration =  $10^{10}$  PFU/mL) and stored at  $4^\circ\text{C}$  before use.

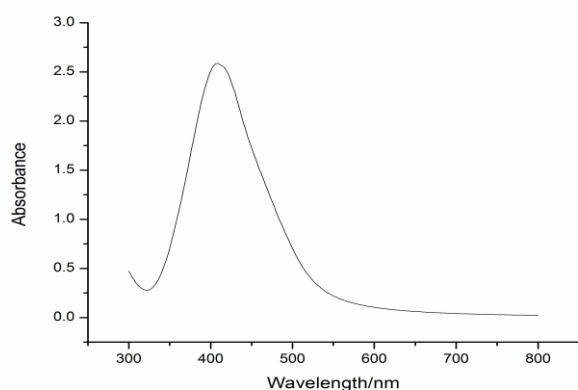


**Fig. 1.** UV-Vis spectrum of silver nanoparticles

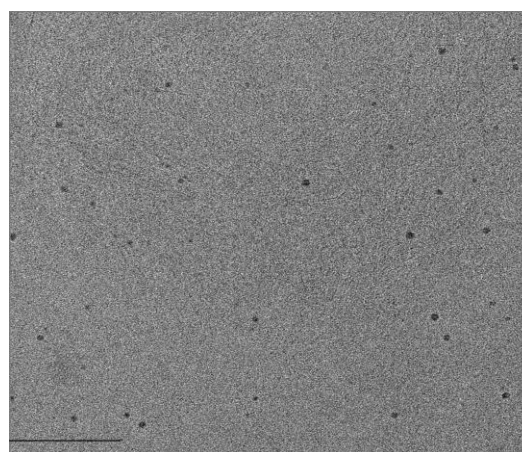


**Fig. 2.** TEM image of silver nanoparticles (black line=200 nm)

The obtained AgNPs and MS2 were characterized using DLS and zetasizer (Fig. 3 and Fig. 6). UV-Vis spectroscopy was used to identify formation of AgNPs (Fig.1 and Fig. 2). The particle size distribution and TEM image were obtained to identify the formed MS2 virus (Fig. 4 and Fig. 5). In brief, 1 mL AgNPs or MS2 were transferred into the cuvette and placed in the zetasizer. Zeta potential and particle size was measured at  $25^\circ\text{C}$ . Similarly, particle size and zeta potentials of AgNPs-MS2 mixture was also characterized (Table 1).

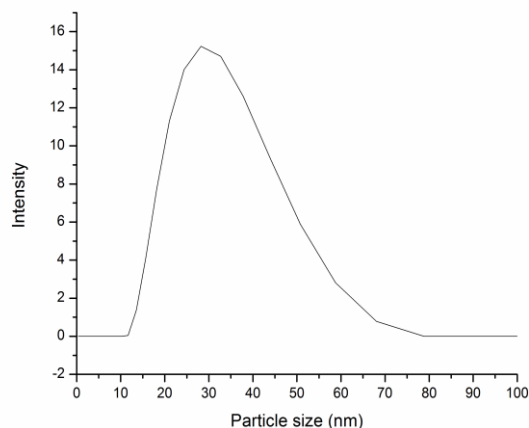


**Figure 3.** Particle size distribution of silver nanoparticles

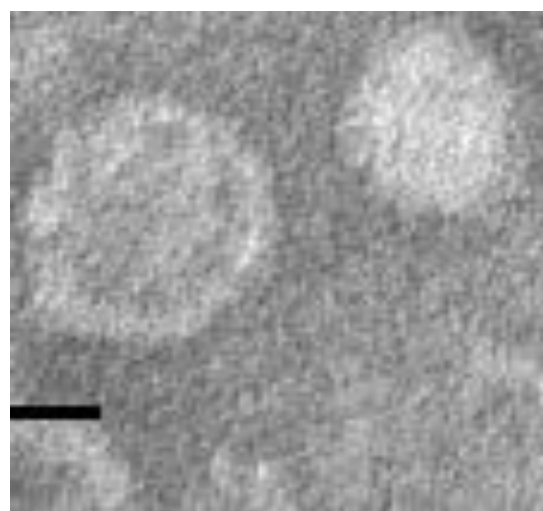


**Figure 4.** TEM image of MS2 bacteriophage (left image; black bar=10 nm)

Toxicity of AgNPs on MS2 virus was quantified by adding aliquots of AgNPs into 100  $\mu$ L MS2 solution to obtain the final total silver concentration of 1, 10, 50, and 100 mg/L. MS2 was exposed to AgNPs for 2 h. The viability of the MS2 was measured using DAL technique as previously described.

### 3 Results and discussion

#### *Characterization of AgNPs and MS2*

As shown in Table 1, average hydrodynamic size of AgNPs and MS2 were measured as 30.5 and 27.5, respectively. TEM images (Fig. 2 and Fig. 3) revealed that mean AgNPs and MS2 sizes of 27.2 nm and 25.6 nm, respectively. The slight differences are due to the aggregation occurred in the solution.

**Table 1** Average particle size and zeta potential of AgNPs and MS2 in DI water

	Average hydrodynamic size (nm)	Zeta potential (mV)
AgNPs	30.5 $\pm$ 1.2	-36.5 $\pm$ 0.6
MS2	27.5 $\pm$ 0.4	-26.8 $\pm$ 0.8
AgNPs-MS2	33.8 $\pm$ 3.6	-32.1 $\pm$ 2.6

#### *Kinetic study on the toxicity of AgNPs on MS2 bacteriophage*

A kinetic study was first conducted using AgNPs at the concentration of 100 mg/L (Fig. 6). The highest AgNPs was chosen because it can show the deactivation kinetic more clearly. As can be seen in Fig. 6, the viability of MS2 bacteriophage decreased over time. The result is consistent with previous studies, which reported similar pattern on the deactivation of virus and bacteria using AgNPs.

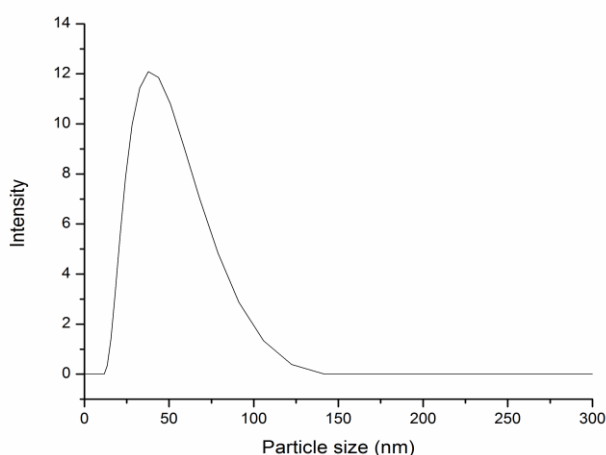


**Figure 5.** Particle size distribution of MS2 virus using DLS technique

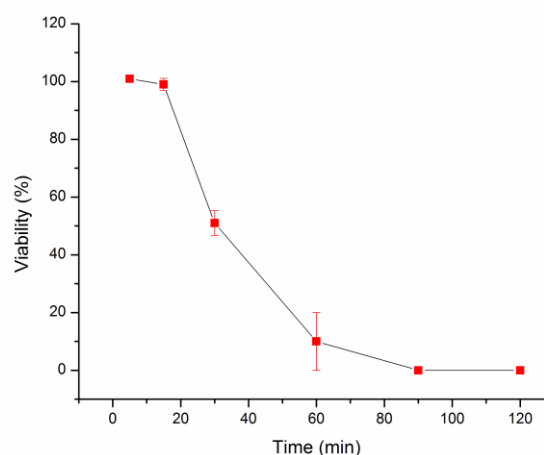


**Figure 6.** Deactivation kinetics of AgNPs on MS2 bacteriophage (Duration=2 h)

#### *Dose-dependent toxicity evaluation*

MS2 bacteriophage was exposed to AgNPs at various concentrations for 2 h. At low AgNP concentration (1 mg/L), the viability of MS2 bacteriophage did not change significantly (Fig. 7). The viability of MS2 bacteriophage began to decrease at 10 mg/L AgNPs. At the highest AgNP concentration (100 mg/L), MS2 bacteriophage was completely deactivated. When AgNP concentration is low, there are low chances that AgNPs can interact with MS2 bacteriophage. However, at high AgNP concentration, more AgNPs can be dispersed in the solution and the chances of the AgNP-MS2 interaction is higher, which result in lower viability of MS2 bacteriophage. The AgNP-MS2 interaction is further confirmed by TEM image taken from the AgNP-MS2 mixture (Fig. 8). As shown in this figure, MS2 bacteriophage is surrounding the AgNP cluster. Previous studies proposed that the toxicity of AgNPs on virus is mainly attributed to the interaction of AgNPs with the sulfur containing proteins of the virus [12-21]. This type of reaction can lead to deactivation of MS2 bacteriophage and decrease its infectivity on the host bacteria cells [17]. Similar findings were reported by previous published studied on HIV virus, Herpes Simplex Virus, and Tacaribe virus. This dose-dependent response pattern indicates that AgNPs can be used as an antiviral reagent.

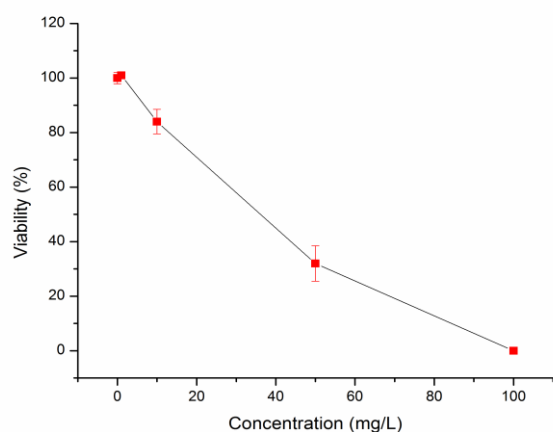


**Figure 7.** Dose-dependent toxicity of AgNPs on MS2 bacteriophage

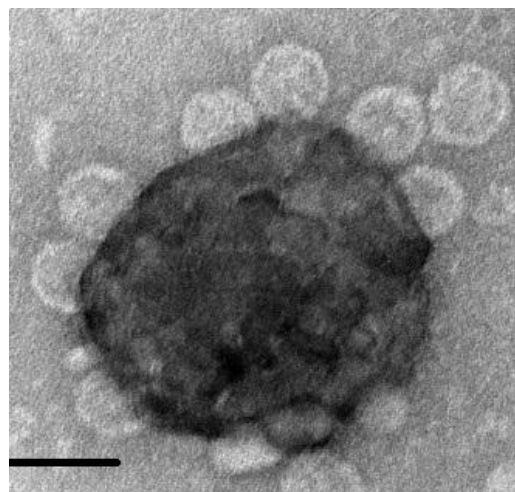


**Figure 8.** Interaction between AgNPs and MS2 bacteriophage

### Conclusion

This work is the first study on toxicity of AgNPs on MS2 bacteriophage. This study shows that both the synthesized AgNPs and the cultivated MS2 bacteriophage are in nanosize range and exhibited negative surface charge. The toxicity of AgNPs on MS2 bacteriophage is dose-dependent, indicating that AgNPs can possibly be used as antiviral reagent in medical and water treatment fields [22, 23].

### References

1. Choi O., Deng K., Kim J., Ross L., Surampalli Y., Hu Z., *Water Res.*, 42 (2012) 3066
2. Zhang H., Oyanedel-Craver V., *J. Environ. Eng.*, 138 (2011) 58
3. Gao J., Youn S., Hovsepyan A., *Environ. Sci. Technol.*, 43 (2009) 3322
4. Zook J., MacCuspie R., Locascio L., *Nanotoxicology*, 19 (2011) 842
5. Kvitek L., Vanickova M., Panacek A., *J. Phys. Chem.*, 113 (2009) 4296
6. Chen S-F., Zhang H., *Adv. Nat. Sci.: Nanosci. Nanotechnol.*, 3 (2012) 035006
7. Fabrega J., Fawcett S., Renshaw J., *Environ. Sci. Technol.*, 43 (2009) 7285
8. Zhang H., Smith J., Oyanedel-Craver V., *Water Res.*, 46 (2012) 691
9. Jin X., Li M., Wang J., *Environ. Sci. Technol.* 44 (19) (2010) 7321
10. Sondi I., Salopek-Sondi J. *J. Colloid Interf. Sci.* 275 (2004) 177
11. Chen S., Zhang H., *Asian J. Chem.*, 25 (2013) 2886
12. Baram-Pinto D., Shukla S., Perkas N., Gedanken A., Sarid R., *Bioconjugate Chem.* 20 (2009) 1497
13. Chen S., Zhang H., *Asian J. Chem.*, 25 (2013) 2909
14. Vijayakumar P., Prasad B., *Langmuir*, 25 (2009) 11741
15. Badireddy A., Hotze E., Chellam S., Alvarez P., Wiesner M., *Environ. Sci. Technol.*, 41 (2007) 6627
16. Gutierrez L., Mylon S., Nash B., Nguyen T., *Environ. Sci. Technol.*, 44 (2010) 4552
17. Liga M., Bryant E., Colvin V., Li Q., *Water Res.*, 45 (2011) 535
18. Bhattacharya R., Mukherjee P., *Adv. Drug Deliver. Rev.*, 60 (2008) 1289
19. Ditto A., Shah P., Yun Y., *Expert Opin. Drug Deliv.*, 6 (2009) 1149
20. Lara H., Ixtepan-Turrent L., Trevino E., Singh D., *J. Bionanotech.*, 9 (2011) 38
21. Mastro M., Hardy A., Boasso A., Shearer G., Eddy C., Kub F., *Med. Chem. Res.*, 19 (2010) 1074
22. Pham M., Mintz E., Nguyen T., *J. Colloid Interf. Sci.*, 338 (2009) 1
23. Zhang H., Oyanedel-Craver V., *J. Hazard. Mater.*, 260 (2013) 272

(2014) ; <http://www.jmaterenvironsci.com>